Calcium Alone Does Not Fully Activate the Thin Filament for S1 Binding to Rigor Myofibrils

Darl R. Swartz,* R. L. Moss,# and M. L. Greaser§

*Department of Anatomy, Indiana University Medical School, 635 Barnhill Drive, Indianapolis, Indiana 46202; #Physiology Department, University of Wisconsin Medical School, Madison, Wisconsin; and §Muscle Biology Laboratory, University of Wisconsin, Madison, Wisconsin, USA

ABSTRACT Skeletal muscle contraction is regulated by calcium via troponin and tropomyosin and appears to involve cooperative activation of cross-bridge binding to actin. We studied the regulation of fluorescent myosin subfragment 1 (fS1) binding to rigor myofibrils over a wide range of fS1 and calcium levels using highly sensitive imaging techniques. At low calcium and low fS1, the fluorescence was restricted to the actin-myosin overlap region. At high calcium and very low fS1, the fluorescence was still predominantly in the overlap region. The ratio of nonoverlap to overlap fluorescence intensity showed that increases in the fS1 level resulted in a shift in maximum fluorescence from the overlap to the nonoverlap region at both low and high calcium; this transition occurred at lower fS1 levels in myofibrils with high calcium. At a fixed fS1 level, increases in calcium also resulted in a shift in maximum fluorescence from the overlap region to the nonoverlap region. These results suggest that calcium alone does not fully activate the thin filament for rigor S1 binding and that, even at high calcium, the thin filament is not activated along its entire length.

INTRODUCTION

Muscle contraction results from ATP-driven cyclical interactions of myosin heads with the actin filament. This process results in a sliding of the actin filaments relative to the myosin-containing thick filaments, giving rise to shortening or force development. In striated muscle, this process is regulated by calcium through regulatory proteins associated with the actin filament, i.e., tropomyosin and troponin (reviewed in Leavis and Gergely, 1984; Chalovich, 1992). Tropomyosin is an elongated dimer that binds along the thin filament and spans seven actin monomers. Troponin binds both actin and tropomyosin in a stoichiometry of one troponin per one tropomyosin per seven actins, comprising the structural unit of the regulated thin filament. The troponin molecule has three subunits, of which the troponin C subunit is the calcium binding protein. The molecular switch for calcium activation involves calcium binding to troponin C followed by complex alterations in thin filament protein-protein interactions, allowing for the interaction of actin and the myosin head (Grabarek et al., 1992).

A steric blocking model was the first widely accepted mechanism by which calcium binding to troponin C might result in thin-filament activation (Haselgrove, 1973; Huxley, 1973; Parry and Squire, 1973; reviewed in Squire, 1994). Calcium binding to troponin was thought to result in an azimuthal movement of tropomyosin on the thin filament from a position that blocks myosin binding to actin to a position that no longer blocks the myosin-actin interactions. This model was based on modeling of x-ray diffraction data from muscle fibers and was further supported by time-resolved x-ray diffraction studies which showed that the proposed structural change preceded force development (Kress et al., 1986). A comparative x-ray diffraction study of oriented regulated thin-filament gels and muscle fibers showed that, in the oriented filaments, the calcium-induced movement of tropomyosin was about 30% of that observed in activated muscle, suggesting that calcium alone results in some movement of tropomyosin, but full movement requires myosin head binding to the filament (Popp and Maéda, 1993). More refined modeling of x-ray data from oriented actin-tropomyosin gels (troponin-free) using the atomic model of F-actin suggests that tropomyosin would still partially block myosin head binding to actin (Lorenz et al., 1995) and supports the idea that additional movement of tropomyosin occurs upon head binding. These structural studies provide strong support for a model of regulation that, at least in part, contains a steric blocking component in which the binding of the myosin head to actin is prevented by tropomyosin.

Another model, in which regulation was through a kinetic mechanism, has been based primarily on steady-state binding studies with regulated thin filaments and S1 (Chalovich, 1992). In this model calcium regulation involves the acceleration of a kinetic transition, thought to be P_i release, in the actomyosin ATPase cycle (Chalovich and Eisenberg, 1982; Chalovich et al., 1981). Single-fiber studies have provided additional support for this model by showing that kinetics of force development were influenced by calcium (Brenner, 1988).

Thus, two different models have been proposed for the regulation of contraction: a steric mechanism that would influence the number of cross-bridge interactions (amplitude) and a kinetic mechanism that would influence the rate of cross-bridge interactions. Additional models have been

Received for publication 4 December 1995 and in final form 28 June 1996.

Address reprint requests to Dr. Darl R. Swartz, Indiana University Medical School, Department of Anatomy, 635 Barnhill Drive, Indianapolis, IN 46202. Tel.: 317-274-8188; Fax: 317-278-2040; E-mail: dswartz@ indyvax.iupui.edu.

0006-3495/96/10/1891/14 $2.00

proposed that incorporate both a steric component and a kinetic component (Rosenfeld and Taylor, 1987; McKillop and Geeves, 1993) to the regulatory mechanism.

A more recent model of thin-filament regulation employs three different states of the thin filament: a blocked state that cannot readily bind S1, a closed state that can bind S1 but only weakly, and an open state that can bind S1 with high affinity (McKillop and Geeves, 1993; Head et al., 1995). In this model, calcium alone shifts the thin filament from the blocked to the closed state, whereas strong binding of S1 shifts the thin filament from the blocked state through the closed state to the open state, and this latter transition is facilitated by calcium and associated with force production. This model was based upon both kinetic and equilibrium binding studies and has some attractive features relative to many of the observed characteristics of the thin filament. The model incorporates a steric component (blocked to closed transition) and a kinetic component (closed to open transition). The blocked to closed transition is likely regulated by the calcium-induced tropomyosin movement described by Popp and Maéda (1993) for regulated thin filaments in the absence of S1. The closed to open transition corresponds to the additional movement detected in muscle fibers (i.e., with myosin heads).

An important feature of the three-state and two-state models is that calcium alone does not result in full activation of the thin filament (open or on state); full activation requires strong S1 binding (Hill et al., 1980; McKillop and Geeves, 1993). This was demonstrated in solution studies using pyrene-labeled tropomyosin (Ishii and Lehrer, 1987) and ATPase activity as a function of S1 concentration (Lehrer and Morris, 1982). These observations have led to the proposal that calcium facilitates activation of the thin filament by allowing S1 binding (Lehrer, 1994).

A simple test of whether Ca^{2+} and strongly binding cross-bridges influence the binding of the myosin head to the thin filament is to incubate rigor myofibrils with a fluorescently labeled S1 and observe the location of S1 binding using fluorescence microscopy. This approach incorporates the native structure of the thin filament and the three-dimensional organization of the thin and thick filaments present in the intact myofibril. A simple prediction is that the S1 will bind preferentially to the highest affinity actin sites (i.e., on or open states) in the myofibril and thus will demonstrate regions where the thin filament is activated. Previously we demonstrated that calcium influences the location of fluorescent S1 binding in rigor myofibrils; without calcium, binding was favored in the overlap region, whereas with calcium, binding was favored in the I-band (Swartz et al., 1990). The location of binding of fluorescent S1 without calcium was dependent upon the S1 level: high levels favored binding in the I-band, whereas low levels favored binding in the overlap. However, the location of binding with calcium was not dependent upon the S1 level, suggesting that calcium alone can activate the thin filament. One difficulty with these studies was that the level of fluorescent S1 required to obtain high-quality micrographs may have resulted in activation of the thin filament by S1 binding, even in the presence of calcium (i.e., the S1 both perturbed the thin filament and indicated its status). If this were true, our previous results suggesting that calcium alone can fully activate the thin filament for rigor S1 binding were incorrect. To address this issue, we have done experiments at a variety of Ca^{2+} concentrations and a wide range of fluorescent S1 levels (ratios between 1:65,000 and 1:2 fluorescent S1:myofibrillar actins). These studies were facilitated by using the high sensitivity and wide dynamic range of a cooled charge-coupled device (CCD) for digital imaging. This allowed detection of fluorescent S1, even at extremely low, and likely nonperturbing, levels.

MATERIALS AND METHODS

Protein purification and modification

Myofibrils, actin, and S1 were isolated from bovine cutaneous trunci muscle. Isolation of myofibrils from rigor muscle was done as described previously (Swartz et al., 1993). Actin was purified as described by Pardee and Spudich (1982). Subfragment 1 was prepared from myosin using chymotrypsin as described by Weeds and Pope (1977), and the A1 isoform was purified using cation exchange chromatography on SP-Sephadex C-50 as described by Swartz and Moss (1992). Labeling of S1 with thiol-specific dyes on SH groups other than SH1 or SH2 was done as described previously (Swartz et al., 1990), with minor modifications. After protecting SH1 and SH2 by 5,5′-dithio-bis-2-nitrobenzoic acid oxidation, the protein was dialyzed against 100 mM KCl, 5 mM HEPES (pH 7.4), 1 mM EDTA at 4°C, followed by mixing with 2 mol of rhodamine-X-maleimide per mol S1 (4.5 mg protein/ml). After incubation at 4°C for 24 h, the reaction was quenched by the addition of dithiothreitol (DTT) to a final concentration of 2 mM. Functional S1 was purified by mixing the conjugated S1 with actin using 3 mol actin/mol S1 in 50 mM KCl, 20 mM Tris (pH 7.6), 1 mM EGTA, and the solution was centrifuged at 150,000 × g for 1 h to pellet acto-S1. The pellets were resuspended in 150 mM KCl, 10 mM KPO_4 (pH 7.2), 10 mM PP_i, 2 mM $MgCl_2$, 2 mM EGTA, 1 mM ATP, 1 mM NaN_3, 1 mM DTT and then centrifuged at 150,000 × g for 1.5 h. The supernatant, containing rhodamine-X-maleimide-conjugated S1 (fS1) and some contaminating actin, was adjusted to final concentrations of 0.3 M NaCl and 2 mM ATP by the addition of solid NaCl and concentrated ATP solutions, respectively. Solid $(NH_4)_2SO_4$ was added to 42% saturation; the solution was mixed for 20 min and then centrifuged at 10,000 × g for 20 min to remove actin contamination. The supernatant was collected and made to 75% saturation with $(NH_4)_2S0_4$. The mixture was stirred for 20 min and then centrifuged at 10,000 × g for 20 min. The resulting pellet was collected and stored at 4°C. Before use, the fS1 was dialyzed against a pCa 9.0 solution (see Solutions section below) containing 1 mM DTT, and filtered through a 0.45-μm filter.

Binding experiments

Myofibrils were washed twice with pCa 9.0 buffer containing 1 mM DTT and 1 mg bovine serum albumin (BSA)/ml. The myofibrils were adjusted to 1 mg/ml in different pCa solutions (9.0, 7.0, 6.0, 5.0, 4.0), and 100 μl was mixed with 300 μl of the same selected pCa buffer containing 1 mM DTT, 1 mg BSA/ml, and different levels of fS1. The solution was incubated in the dark for 4 h at room temperature and then centrifuged for 10 s at 13,500 × g. The supernatant was removed and the pellet resuspended in 300 μl of the proper pCa buffer; 100 μl was spread on a coverslip before fixation for 15 min with 3% formaldehyde in the proper pCa buffer. The coverslip was rinsed in 75 mM KCl, 10 mM imidazole (pH 7.2), 2 mM $MgCl_2$, 2 mM EGTA, 1 mM NaN_3, drained, and then mounted in 75% glycerol (v/v), 75 mM KCl, 20 mM Tris (pH 8.5), 2 mM $MgCl_2$, 2 mM

EGTA, 1 mM NaN_3, 1 mg phenylenediamine/ml. Coverslips were sealed to slides with nail polish. After drying, slides were stored at −20°C before microscopic imaging.

The concentration of myofibrils (0.25 mg/ml) was constant for all conditions, and the fS1 was changed to give different ratios of A:fS1. A wide range of fS1 levels was used for the binding experiments, and the ratio of S1 levels relative to the estimated total actin present in the myofibrils was estimated based upon the value of 5.4 μmol/g myofibrillar protein (Yates and Greaser, 1983). The levels are expressed relative to the myofibrillar actin (1.35 μM) and ranged from 2 A:1 fS1 to 65,500 A:1 fS1 (i.e., 0.68 μM fS1 to 21 pM fS1).

Solutions

Buffers of different calcium concentration were made by mixing stock solutions of pCa 9.0 and 3.0. The base solution was 20 mM piperazine-*N,N'*-bis(2-ethanesulfonic acid (pH 7.0), 4 mM $MgCl_2$ (free), 4 mM EGTA, 1 mM NaN_3, KCl to yield 180 mM ionic strength, and $CaCl_2$ to yield the desired free calcium concentration. The stability constants listed by Godt and Lindley (1982) and Fabiato's program (1988) were used to determine the concentrations of total $MgCl_2$ and $CaCl_2$ needed to achieve the desired free ion concentrations.

ATPase assays

Myofibrils (final concentrations of 0.125 mg/ml) were mixed with different pCa buffers (1 mg BSA/ml, 1 mM DTT), and the reaction was started by the addition of ATP to a final concentration of 2 mM. After different times of incubation at 23°C, the reaction was quenched by the addition of trichloroacetic acid to a concentration of 2.3% followed by centrifugation at 13,500 × *g* for 15 s. The P_i in the supernatant was determined by the assay of Carter and Karl (1982). The rate of P_i generation was determined from single time point assays after correcting for P_i contamination in the buffer. The rate data were corrected for the rate at pCa 9.0 to yield the calcium-dependent activity, which was normalized to the rate at pCa 4.5. The rates were determined in triplicate for each pCa level.

Imaging

Myofibril images were acquired with a Nikon Diaphot equipped with a phase-contrast 100× (NA 1.4) oil-immersion lens, 100-W epifluorescence illumination, and Texas Red fluorescence filter. Digital images were obtained using a CCD camera (Thomson 7883 chip; Photometrics, Tuscon, AZ) controlled by a Matrox board in a Macintosh IIfx with Nu 200.2 software (Photometrics). For fluorescence imaging, exposure times were varied to yield a minimum dynamic range of 300 intensity units (max-min); for extremely low levels of fS1 the gain was increased from 1 to 4. The longest exposure times were 15 s. Three to eight different myofibrils were imaged for each combination of pCa and [fS1], and the images were obtained by first acquiring the phase contrast image and then the fluorescence image. No adjustment in focus was made between collections of the phase contrast and fluorescence images. The digital images were subsequently processed with IPLab Spectrum software (v2.5; Signal Analytics Corp., Vienna, VA). The fluorescence intensity data of the region of interest (ROI) containing a myofibril segment (four or five sarcomeres) in the same plane of focus was normalized in 16 bits (min and max of the ROI) and converted to 8 bits before construction of the phase and fluorescence image montages. Thus, each fluorescence image utilizes the maximum dynamic range within the specific ROI to demonstrate the relative fluorescence levels. Whenever possible, montages were made from myofibrils of similar sarcomere length. The montages were made with a Z-line in the center of the myofibril image, so that comparison of sarcomere length could be made by inspecting the image edge and to aid in comparisons of different myofibrils.

Fluorescence intensity ratios were obtained from different regions of a sarcomere. The 12-bit non-normalized image data were digitally enlarged fourfold by using bilinear interpolation (IPLab software). A rectangular region of interest (10 × 20 pixels, 0.22 × 0.45 μm) was selected near the myofibril image edge, and the average intensity was measured. This value was used to correct for background fluorescence intensity. Subsequently, a fluorescence intensity profile was recorded to determine the pixel positions of the Z-lines of three consecutive sarcomeres. A rectangular ROI in the center of the myofibril (10 × 20 pixels) spaced 0.34 μm from the Z-line (center-to-center), with the long axis perpendicular to the long axis of the myofibril, was selected, and the average fluorescence intensity value of the region was measured to yield the intensity in the nonoverlap region. The same-sized ROI was spaced 1.02 μm from the Z-line (center-to-center) to yield the overlap region fluorescence intensity. The nonoverlap and overlap region fluorescence intensity values for each half-sarcomere were corrected for background fluorescence; then the nonoverlap-to-overlap ratio was determined.

Quantitative measurement of fS1 binding to myofibrils

The amount of fS1 bound to myofibrils was measured both by biochemical methods and by imaging methods using fluorescence intensity. For the biochemical approach, 25 μl of myofibrils (1 mg/ml) was mixed with 75 μl of different concentrations of fS1 in either pCa 4.0 or 9.0 solution containing 1 mM DTT and 1 mg/ml BSA and was incubated at room temperature for 4 h. Myofibrils were pelleted by centrifugation at 13,000 × *g* for 1 min, and then 75 μl of the supernatant was removed for assay of free fS1 using NH_4/EDTA ATPase activity (Swartz and Moss, 1992). Samples with buffer instead of myofibrils were processed in the same fashion and assayed for NH_4/EDTA ATPase activity to determine the total fS1. Bound fS1 was determined by subtracting free activity from total activity. Myofibril samples without fS1 were processed in the same fashion to correct for residual myofibrils in the supernatant. The NH_4/EDTA ATPase activity was measured in 0.4 M NH_4Cl, 40 mM EDTA/Tris, 25 mM Tris (pH 7.0), and the reaction was started by adding ATP to 2 mM final. The activity was stopped by the addition of 10% trichloroacetic acid, and the protein was pelleted by centrifugation at 13,000 × *g* for 15 s. The supernatant was assayed for P_i as described above for myofibrillar ATPase activity.

The amount of fS1 bound to the myofibrils was determined directly by measuring the fluorescence intensity of sarcomeres in myofibrils incubated with fS1 at pCa 4.0 or 9.0 at fS1 levels of 32 A:1 fS1 (42 nM) and 64 A:1 fS1 (21 nM). Myofibrils (25 μl of 1 mg/ml) were mixed with fS1 (75 μl), incubated, and processed for imaging as described for binding studies, except that 100 μl was used for resuspension. For measurement of fS1 fluorescence intensity, myofibrils were imaged as described above, but using a Photometrics CCD (KF 1300 chip) attached to a Zeiss Axiovert TV microscope equipped with a 100× (1.3 NA) oil immersion lens, a narrow bandpass Texas Red filter, and a 100-W mercury lamp. Fluorescence images were obtained using a 0.4-s exposure for all conditions. For fluorescence intensity measurements, the myofibril within the image was rotated to the vertical using bilinear interpolation and cropped to obtain a minimum of three sarcomeres, with the myofibril in the center of the cropped image. The cropped image was corrected for background intensity by subtracting the image minimum value from the image data. The net intensity image was then analyzed using segmentation analysis with IPLab Spectrum software. To properly segment the sarcomeres, a 2 × 50 pixel ROI (intensity set at 0) was pasted at the Z-line (determined from the phase image) to separate adjacent sarcomeres. This image was then segmented from 10% of maximum intensity to maximum intensity. The mean intensity for each segment (sarcomere) was measured and used to determine the sarcomeric fluorescence intensity. A minimum of three contiguous sarcomeres were used to calculate the mean intensity per myofibril, and 13–22 myofibrils were used to calculate the mean intensity for each pCa/fS1 level. Myofibrils were selected based upon phase image quality to minimize operator bias.

Time course of fS1 distribution

To test whether incubation time had an influence on the distribution of fS1, and whether 4 h was long enough to reach the steady-state distribution of fS1 throughout the sarcomere, a time course experiment was conducted. One difficulty with this experiment is deciding which pCa and fS1 conditions should be used. The selected conditions should have very low fS1 and a pCa in which a pattern shift is likely. As a compromise, pCa 4.0 and a fS1 level of 512 A:1 fS1 (2.6 nM) were used. Myofibrils were mixed with fS1 as described for binding experiments, and at timed intervals, samples were processed for imaging as described above. Sampling started at 4 min, and subsequent samples were taken at twice the previous interval. Images were obtained as described above, but with a 4-s exposure for all fluorescence images. The distribution of fS1 was determined using the nonoverlap/overlap fluorescence intensity ratio described above and plotted as a function of time.

Other biochemical procedures

Myofibril protein concentration was estimated using the biuret assay (Gornall et al., 1949), with BSA as the standard. The fS1 protein concentration was estimated with the microtannin assay of Mejbaum-Katzenellenbogen and Dobryszycka (1959), using unlabeled S1 as a standard. Actin and S1 concentrations were estimated by UV absorbance, using mass absorptivities of 1.17 and 0.75 ml/mg-cm at 280 nm and molecular weights of 43,000 and 120,000. The labeling ratio was estimated using a molar absorptivity of 70,000/M-cm at 580 nm. The labeling ratio was 1.0 for the preparation used in this study. Note that the labeling ratio is a population average and that the individual molecules of S1 could have 0, 1, 2 mole dye/mole protein, giving a population average of 1 mole dye/mole S1. Protein purity was monitored by sodium dodecyl sulfate-polyacrylamide gel electrophoresis as described by Fritz et al. (1989). Rhodamine-X-maleimide was purchased from Molecular Probes (Eugene, OR); other reagents were from Sigma Chemical Co. (St. Louis, MO).

RESULTS

ATPase activity

Bovine *cutaneous trunci* myofibrils were used because they have longer thin filaments than rabbit psoas myofibrils (Swartz et al., 1993), therefore allowing wider regions of the overlap and nonoverlap areas of the sarcomere to be imaged. The calcium dependency of the myofibrillar ATPase has not been characterized for these myofibrils, and thus initial experiments were done to determine the relative ATPase activity as a function of pCa. These measurements allow the determination of the degree of calcium regulation (relative increase in activity caused by calcium) as well as the calcium level for half-maximum activation and a cooperativity parameter (Hill coefficient) by fitting the data to the Hill equation. The degree of activation [(pCa 4.5 rate–pCa 9.0 rate)/pCa 9.0 rate] was 16.7, showing that calcium activation was well preserved in the myofibrils. The data in Fig. 1 show that the ATPase activity–pCa relation exhibits cooperation with a Hill coefficient of 2.92 and half-maximum activation at pCa 6.0. These values are similar to those obtained from rabbit psoas myofibrils under similar conditions (Zot and Potter, 1987). The pCa required for maximum activation of ATPase activity was 5.4 or lower. Thus, by this enzymatic measure of thin-filament activation, the thin filament was fully "on" at pCa levels below 5.4. If this measure of activation is equivalent to that measured by the pattern of fS1 binding, the pattern should be independent of [fS1] when pCa is less than 5.4, if calcium alone fully activates the thin filament.

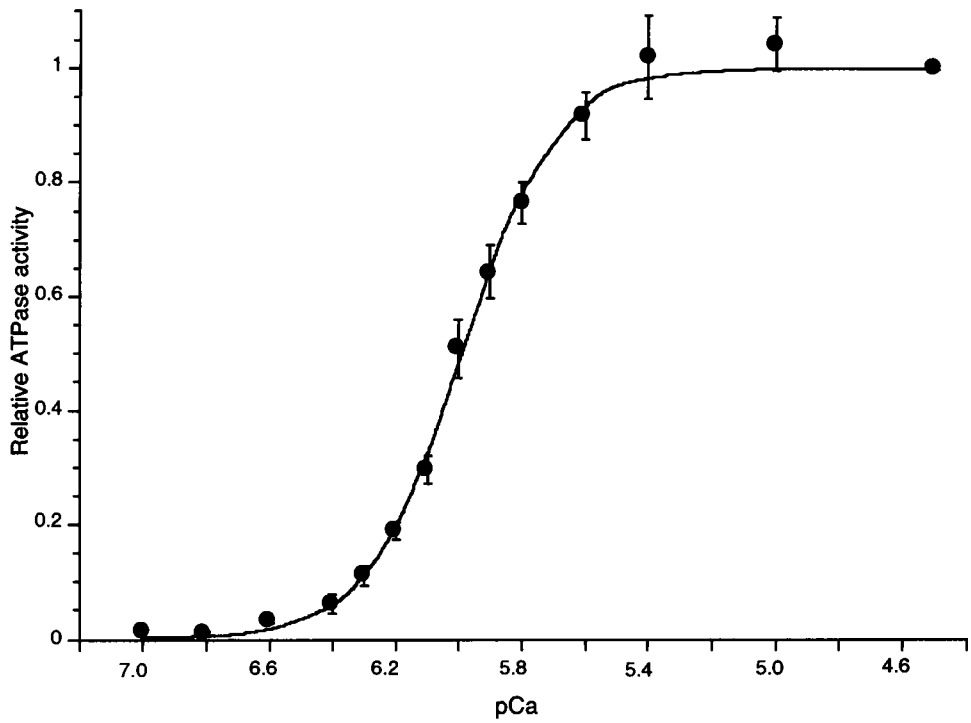

FIGURE 1 Relative ATPase activity–pCa relation for bovine myofibrils. Myofibrils were mixed with buffer solutions of varying pCa, and the reaction was started by the addition of ATP to a final concentration of 2 mM. Data points represent the mean (±SD) of triplicate assays (corrected for activity at pCa 9.0) relative to the activity at pCa 4.5. The average ATPase activity at pCa 4.5 was 0.11 nmol $P_i/\mu g \cdot min$, and at pCa 9.0 it was 0.0062 nmol $P_i/\mu g \cdot min$. The smooth line represents the best fit of the data to the Hill equation, with half-maximum activity at pCa 6.0 and $n = 2.92$.

Binding of fluorescent S1

Fluorescent S1 binding studies were conducted using levels of fS1 that were subsaturating with respect to total myofibrillar actin. Thus the distribution of the fS1 within the sarcomere localizes the highest affinity sites, assuming that the 4-h incubation time allowed for equilibration of fS1 within the myofibrils. There are two simple hypotheses that can be made about the distribution of fS1 within the sarcomere: 1) all actin sites have the same affinity for fS1, or 2) not all actin sites have the same affinity for fS1. If the first hypothesis is true, the pattern of fluorescence would localize the sites not occupied by intrinsic myofibrillar myosin heads and thus would give rise to a pattern with more fluorescence in the I-band and less in the overlap region. Such patterns would give a nonoverlap/overlap region intensity ratio of 2 based upon the calculated number of available sites in these two different regions (Swartz et al., 1993). If the second hypothesis is valid, fS1 binding will reveal the highest affinity sites, thereby localizing these sites within the sarcomere and yield differing nonoverlap/overlap ratios.

fS1 binding at very low concentration

The difficulty with using S1 binding to study the state of thin-filament activation is that S1 binding itself activates the thin filament (Bremel and Weber, 1972; Murray et al., 1981; Swartz et al., 1990). This activation is dependent upon S1 concentration; however, if a low enough S1 concentration is used, fluorescent S1 will serve as a sensor of the state of the thin filament rather than as an activator. To demonstrate that the imaging system allowed visualization of fluorescent S1 at levels that did not perturb the thin filament, we used extremely low levels of fluorescent S1. Fig. 2 shows paired phase contrast (1P) and fluorescent (1R) images of a myofibril at pCa 4.0 in which fluorescent S1 was added at 65,500 A:1 fS1 (21 pM). This level of S1 corresponds to about 1 fS1 per 138 thin filaments, assuming 473 actins in each 1.3-μm bovine thin filament. The fluorescent image shows punctate spots that likely represent individual fluorescent S1 molecules (approximately 30 fS1 spots per sarcomere should be visible if all fS1 bound to the myofibrils). The different intensities of individual spots were likely caused by differences in the plane of focus and/or differences in conjugation levels (i.e., 1 mol dye/1 mol S1; 2 mol dye/1 mol S1). Further inspection of the image pair in Fig. 2 shows that most of the fluorescence was confined to the overlap region even though the calcium level was well above that needed to maximally activate ATPase activity (see Fig. 1).

When myofibrils were treated with slightly higher [fS1], the fluorescent patterns differed at high and low calcium levels. Fig. 3 shows phase contrast and fluorescent images of myofibrils treated with 16,000 A:1fS1 (84 pM) at pCa 9.0 and pCa 4.0. At pCa 9.0 (1R), the fluorescence was solely in the actin-myosin overlap region, whereas at pCa 4.0 (2R) it was predominantly in the overlap region with some in the I-band. The level of S1 in these experiments is four times that used in Fig. 2, and at pCa 4.0 there were correspondingly more punctate spots. Such spots are not as evident at pCa 9.0, which would be expected if the location of binding of the same number of molecules of fS1 were restricted to a smaller region, i.e., the region of overlap between thick and thin filaments. Measurement of the fluorescence intensity (12 bit, non-normalized data) in same-sized (length and width) sarcomeres of myofibrils treated with the same amount of S1 (2.6 nM, 512 A: 1fS1) and identical exposure conditions showed that the sarcomere fluorescence intensity at pCa 9.0 was 91% of that at pCa 4.0. Thus, calcium had little influence on the amount of fS1 bound, but influenced the location of fS1 binding in the sarcomere.

fS1 distribution at high calcium and various [fS1]

Subfragment 1 itself can perturb thin-filament activation at higher concentrations; this is demonstrated for high calcium

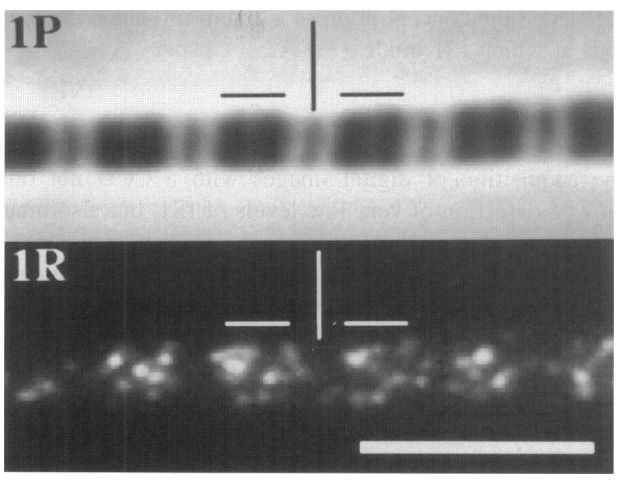

FIGURE 2 Binding of fluorescent S1 to rigor myofibrils at high calcium and extremely low levels of S1. Myofibrils were incubated with 21 pM fS1 (65,500 A:1 fS1) at pCa 4.0 and processed as described in Materials and Methods. Vertical bars mark the Z-line; horizontal bars mark the A-band. P, phase contrast; R, rhodamine fluorescence image. Scale bar, 5 μm.

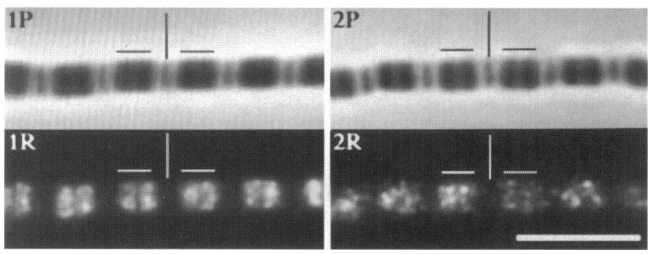

FIGURE 3 Location of fluorescent S1 binding at low and high calcium. Myofibrils were incubated with 84 pM fS1 (16,000 A:1 fS1) at pCa 9.0 (1P and 1R) or pCa 4.0 (2P and 2R). Bars and lettering nomenclature are described in the Fig. 2 legend. Fluorescent S1 binding is more disperse at high calcium concentration. Scale bar, 5 μm.

in Fig. 4. In this figure, the use of four different levels of fS1 resulted in distinctly different binding patterns. At the lowest level (512 A:1 fS1) (Fig. 4, 1R) most of the fS1 was located in the overlap region, and a much smaller amount was in the I-band. At 256 A:1 fS1 (Fig. 4, 2R), most of the fluorescence was in the region of overlap between thick and thin filaments, but the differences in binding between the overlap and I-band region appeared to be less; however, there was a slight preference for fS1 binding just adjacent to the Z-line. Such binding was specific to this level of S1 and calcium concentration, but the reason for enhanced binding adjacent to the Z-line is unknown. When the fS1 level was increased to 64 A:1 fS1 (Fig. 4, 3R), there was little difference in the relative amounts of S1 bound in the overlap region and the I-band. At 8 A:1 fS1 (Fig. 4, 4R), most of the fluorescence was in the I-band and a lesser amount was in the overlap region, as would be expected if all actin sites had the same affinity for S1. Thus, at low levels of fS1 and high levels of calcium, fS1 binding is not random with respect to unoccupied sites on actin, and the pattern of binding was dependent upon the level of fS1.

Influence of calcium on fS1 distribution

In our previous study (Swartz et al., 1990), we used only high and low calcium with different levels of fS1. In the current study, we investigated the influence of graded levels of calcium on the pattern of fS1 binding at a fixed fS1 level. The pattern of fS1 binding was influenced in a graded fashion when [Ca^{2+}] was varied (pCa 7.0, 6.0, 5.0, 4.0) and myofibrils were treated with a constant level of fS1 (32 A:1 fS1). At pCa 7.0 (Fig. 5, 1R), the fS1 was located solely in the overlap region, whereas at pCa 6.0 (Fig. 5, 2R) there was also some fluorescence in the I-band, albeit much less than that in the overlap region. When the pCa was 5.0 (Fig. 5, 3R), the fluorescence image showed a complex pattern in which most of the fluorescence was localized at the A-band–I-band junction, with less fluorescence in the overlap region and the I-band. Similar patterns were also observed with 16 A:1 fS1 at pCa 6.0 and 8 A:1 fS1 at pCa 9.0 and pCa 7.0; the pattern was not observed with any level of fS1 at pCa 4.0 (see Fig. 4). At pCa 4.0, the fS1 was bound mostly in the I-band, with a lesser amount in the overlap region, as shown in Fig. 4, 4R above. Thus, both the level of fS1 and the concentration of calcium influence the locations at which fS1 binds.

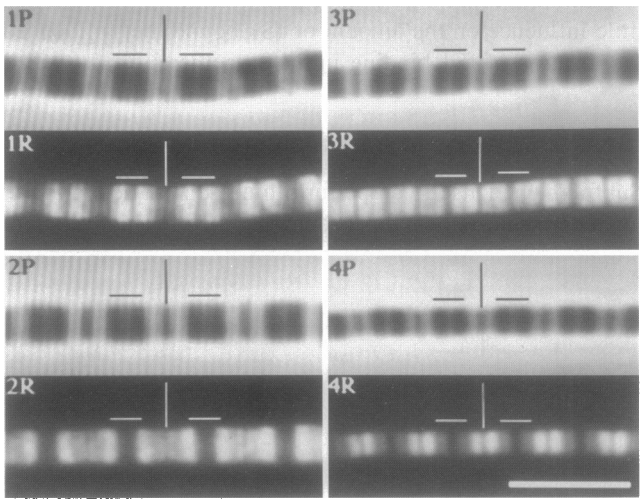

FIGURE 4 Influence of fluorescent S1 concentration on the location of fluorescent S1 binding at high calcium (pCa 4.0). The rhodamine S1 concentrations were 2.6 (1P and 1R), 5.3 (2P and 2R), 21 (3P and 3R), and 170 nM (4P and 4R), corresponding to 512, 256, 64, and 8 A:1 fS1, respectively. Bars and lettering nomenclature are described in the Fig. 2 legend. Fluorescent S1 binding patterns were highly dependent upon the actin-to-S1 ratio. Scale bar, 5 μm.

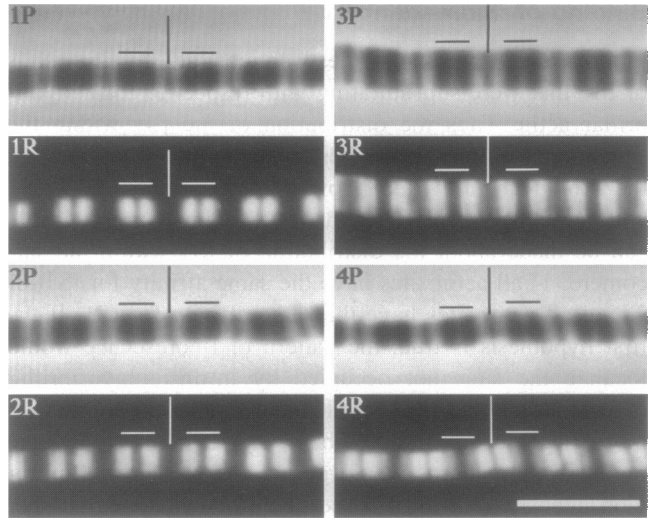

FIGURE 5 Influence of calcium concentration on the location of fluorescent S1 binding. Myofibrils were incubated with 42 nM fS1 (32 A:1 fS1) at pCa 7.0 (1P and 1R), 6.0 (2P and 2R), 5.0 (3P and 3R), and 4.0 (4P and 4R). Bars and lettering nomenclature are described in the Fig. 2 legend. Fluorescent S1 binding converted from localization in the overlap region to an I-band dominant pattern as the calcium concentration was increased. Scale bar, 5 μm.

Quantitative analysis of fS1 distribution

The acquisition of digital images with a CCD not only allowed detection of very low levels of fS1, but also quantitative analysis of the fluorescence intensity data. Fig. 6 shows the fluorescence intensity profiles from sarcomeres of different myofibrils under different conditions. Fig. 6 *A* shows normalized intensity profiles obtained from sarcomeres at pCa 4.0 and either 2.6, 21, or 170 nM fS1. These profiles demonstrate relative differences in fluorescence intensity in the overlap and I-band. At low fS1 (curve 1), most of the fluorescence was in the overlap region, whereas at intermediate fS1 (curve 2), there was little difference between the fluorescence intensities in the overlap and I-band regions. At high fS1 (curve 3), the fluorescence intensity in the I-band peaked in the middle of the I-band region of the half-sarcomere, and the intensity was about

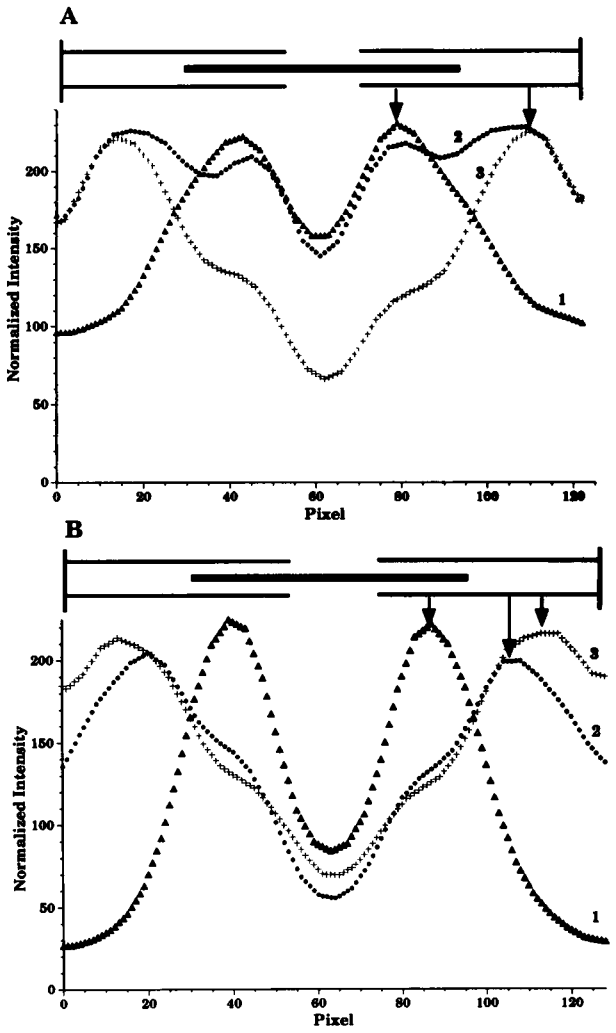

FIGURE 6 Sarcomeric fluorescence intensity profiles at high and low calcium and various fS1 levels. Profiles were obtained from sarcomeres of very similar length by averaging the intensity across the sarcomere. (*A*) Profiles from myofibrils at pCa 4.0 and 2.5 nM (1), 21 nM (2), and 170 nM (3) fS1 are shown with arrows designating intensity peaks. (*B*) Profiles from myofibrils at pCa 9.0 at 42 nM (1), 170 nM (2), and 340 nM (3) fS1 are shown with arrows designating intensity peaks. A diagram of the sarcomere with thin lines representing thin filaments and thick lines representing thick filaments is shown above each graph.

twice that in the overlap region. At low calcium (pCa 9.0, Fig. 6 *B*), similar profiles were observed as the fS1 concentration was varied, with some minor differences. At low fS1 (42 nM, curve 1), the profile showed that fluorescence intensity peaked in the middle of the overlap region and that the intensity approached the baseline in the half-sarcomere I-band region, even though the level of fS1 was relatively high compared to those used to obtain the profiles at pCa 4.0. At intermediate fS1 (170 nM, curve 2), the fluorescence intensity peaked near the I-band–A-band junction. At high fS1 (675 nM, curve 3) it peaked in the middle of the half-sarcomere I-band region. The profile shown for 170 nM was from an image similar to Fig. 5, 3R, in which there was a bright stripe at the I-band–A-band junction. These graphical representations of the relative amount and location of fS1 binding in the sarcomere allow a more quantitative analysis of the images than the actual micrographs.

An additional method to quantitatively evaluate fS1 distribution as a function of calcium and fS1 concentrations is to measure the fluorescence intensity ratio of the nonoverlap and overlap regions. Such a ratio allows comparisons between myofibrils that differ in diameter, incubation, and exposure conditions. As stated earlier, if all sites on actin had the same affinity for fS1, the ratio of I band fluorescence to overlap region fluorescence would be 2. The images shown in Figs. 2–5 demonstrate that under most conditions this was not the case. Fig. 7 plots the fluorescence intensity ratio at pCa 4.0 and pCa 9.0 over a wide range of fS1 levels. The inset illustrates how the ratios were determined. The ratio was measured in three consecutive sarcomeres from two or three myofibrils for each condition and used to calculate the mean values shown in Fig. 7. The mean sarcomere length for the myofibrils was 2.93 μm (range 2.60–3.36 μm). The graph shows that the relationship between the ratio and fS1 concentration was not constant and differed for high and low calcium concentrations. At pCa 4.0 the ratio was about 0.5 at low fS1 concentration and gradually increased as the fS1 concentration was increased. The greatest change in the ratio occurred between 10 and 100 nM fS1. At pCa 9.0 the minimum ratio was 0.2 and was independent of an fS1 level below 50 nM. Between 50 and 120 nM fS1 there was an abrupt increase in the ratio, i.e., the intensity ratio–[fS1] relationship at low Ca^{2+} concentration was switched to higher concentrations of fS1. In both cases, the ratio approached the predicted value of 2 when the fS1 concentration was very high.

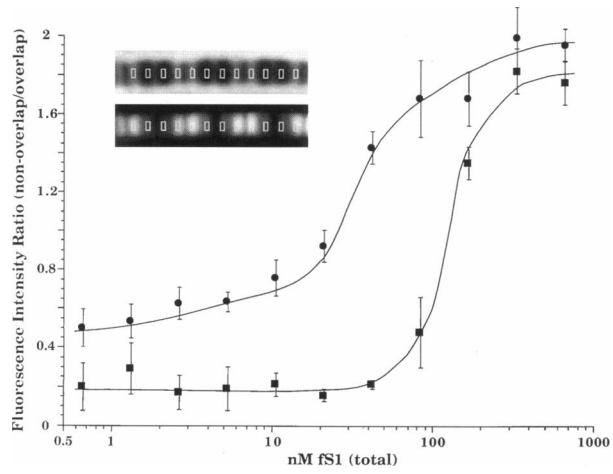

FIGURE 7 Fluorescence intensity ratios (nonoverlap/overlap) for myofibrils at high and low calcium. The 12-bit images were analyzed as described in Materials and Methods to obtain intensity ratios for the different regions. The inset shows images with the ROIs that were used to determine the nonoverlap and overlap intensity values. Ratios were determined for myofibrils at pCa 4.0 (●) and 9.0 (■). Data points represent the mean (±SD) of half-sarcomeres from two or three myofibrils (six half-sarcomeres/myofibril). The curves were drawn by eye.

Quantitative interpretations of the images presented here involve several assumptions about the nature of the fS1 binding to myofibrils. First, we assume that essentially the same amount of fS1 binds to the myofibrils independently of calcium concentration under rigor conditions. Biochemical studies have shown that there is little difference between the binding of rigor S1 to regulated thin filaments with and without calcium (Murray et al., 1981), which supports our assumption. However, the validity of this assumption was directly tested by both biochemical methods and image analysis. The influence of calcium on the amount of fS1 bound to myofibrils was determined by measuring the NH_4/EDTA ATPase activity of fS1 in the supernatants of S1-myofibril mixtures after centrifugation (free fS1) and fS1 without myofibrils (total fS1); the amount of bound fS1 was determined by the difference. A plot of bound fS1 versus free fS1 is shown in Fig. 8. The graph readily shows that calcium did not influence the amount of fS1 bound to myofibrils under rigor conditions over the subsaturating range tested. Additionally, the amount of fS1 bound was determined using image analysis. Myofibrils were incubated at pCa 4.0 or 9.0 and fS1 levels of 64 and 32 A:1 fS1 (corresponding to the two lowest levels of free fS1 in Fig. 8), and fluorescent images were obtained using the same exposure conditions. The average fluorescence intensity per sarcomere was measured using segmentation analysis; the data are shown in Fig. 9. The figure demonstrates that the fluorescence intensity per sarcomere was not influenced by calcium and that a twofold reduction in fS1 resulted in about a twofold reduction in fluorescence intensity per sarcomere (Fig. 9 *A*). Of particular importance is the observation that, although the distribution of fS1 was quite different (Fig. 9 *B*), the total amount of fluorescence emitted per sarcomere was the same.

Second, we assume that there was no fluorescence quenching or enhancement caused by the local environment surrounding the Texas Red fluorochrome. The combination of the biochemical data on fS1 binding and the image analysis data on fS1 binding strongly support this assumption. If there were significant quenching or enhancement, the biochemical and image analysis data would not agree. An additional concern is that of inner filter effects decreasing the measured fluorescence intensity when one considers the high local concentration of fS1 reached in the nonoverlap region at near-saturating levels. If this occurred, the nonoverlap/overlap ratio data would not be as close to the theoretical values as observed.

Third, we assumed that the fS1 was distributed uniformly through the cross section of the myofibril instead of binding only to the surface and that 4 h of incubation was sufficient for steady-state distribution. Images were collected by adjusting the focus to obtain the visually optimal phase-contrast image and then obtaining the fluorescence image without readjusting the focus. The best phase-contrast image is obtained when the focal plane is in the center of the myofibril, and thus the fluorescence image was obtained when the center of the myofibril was in the focal plane. Inspection of Fig. 2, 1R shows that the fluorescence spots had gradations in intensity that most likely represented their positions relative to the focal plane of the lens. Furthermore, we have previously shown (Swartz et al., 1993) that images obtained from myofibrils treated under conditions favoring surface binding of fS1 appear different from any of those in the current work. A further test was done to validate the 4-h incubation by monitoring the intensity ratio as a function of time of incubation with fS1. This analysis tested for development of a steady-state distribution along the length of the thin filaments rather than solely across the myofibril. For this, conditions (pCa 4.0, 512 A:1 fS1) were selected that were most likely to result in a change in pattern (i.e., intensity ratio) with incubation time considering the nature of the thin filament and the poor accessibility of the overlap

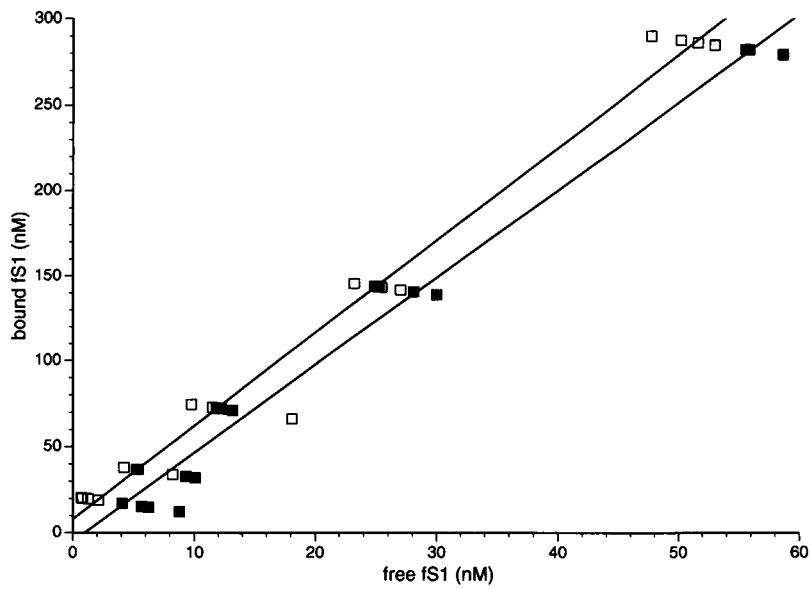

FIGURE 8 Measurement of bound fS1 using ATPase assay. Myofibrils were mixed with different levels of fS1 (from 64 A: fS1 to 4 A: S1) at pCa 4 (■) or 9 (□) and incubated at room temperature for 4 h. After pelleting at 13,000 × *g* for 1 min, supernatants were removed and assayed for free fS1 using NH_4/EDTA ATPase activity. Total activity was measured in samples treated in the same manner, but with the addition of buffer instead of myofibrils. Four samples were measured for each fS1 level. Note that there was little difference in the proportions of fS1 bound at pCa 4 and 9 over the range of fS1 tested.

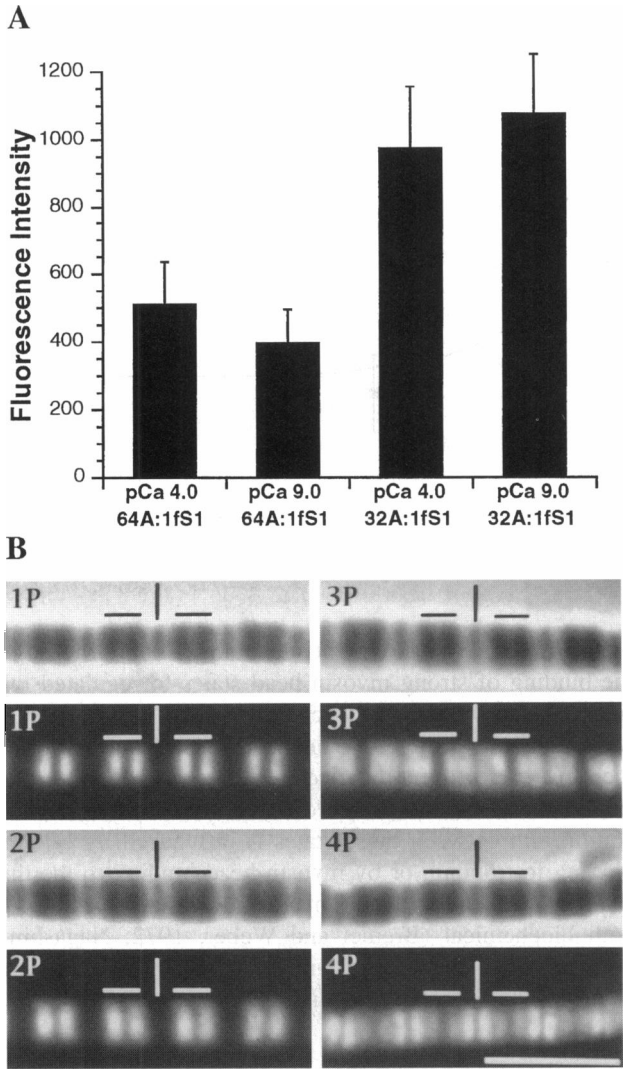

FIGURE 9 Measurement of bound fS1 using fluorescence microscopy. Myofibrils were mixed with two different levels of fS1 [64 A: fS1 (21 nM) or 32 A: fS1 (42 nM)] at pCa 4 or at pCa 9. Samples were processed for imaging as described in Materials and Methods and imaged using the same exposure time for all conditions. (*A*) Histogram showing sarcomeric fluorescence intensity. Bars represent mean of 13–22 myofibrils with standard deviation lines. Note that the fluorescence intensity per sarcomere was very similar at both high and low calcium for each level of fS1 and that the intensity scaled with amount of fS1. (*B*) Montage of representative myofibrils showing the different patterns observed under the various conditions. Myofibrils 1 and 2 were pCa 9.0 at 64 and 32 A: 1 fS1, respectively, and myofibrils 3 and 4 were pCa 4.0 at 64 and 32 A: 1 fS1, respectively. Bars and lettering nomenclature are described in the Fig. 2 legend.

region of the thin filament. Fig. 10 shows the intensity ratio as a function of time over a 256-min incubation period. The curve readily demonstrates that the ratio reached a near-steady-state value within 128 min and had a half-time of about 45 min. The intensity ratio under these conditions was slightly higher than that obtained from the experiments used to generate Fig. 7, but they are within the scatter of the data. Fig. 11 shows the appearance of the fluorescence pattern (and resulting ratio) for times of 4, 8, 16, 32, 64, and 128 min. The change in distribution is readily apparent when comparing 4 min with 128 min (Fig. 11, 1R, 6R), whereas the change between successive time points is less obvious. Thus, incubation of myofibrils with fS1 for 4 h allowed for equilibration of fS1 throughout the myofibril and along the length of the thin filaments.

Fourth, we assume that labeling did not dramatically alter the properties of fS1 in terms of its interaction with actin. In support of this idea, the labeling and isolation procedures do not dramatically alter the kinetic properties of fS1 relative to unlabeled S1 (Swartz et al., 1990). Fifth, we assume that fS1 does not interact nonspecifically with the thick filament. Images presented in the results clearly show that fS1 binding was restricted to the thin filaments because, at longer sarcomere lengths, a wider nonfluorescent region in the center of the A-band was visible (compare Figs. 4, 1R and 2R, and Fig. 5, 1R and 2R).

Finally, we assume that over time, fS1 will bind to the most stable, high-affinity actin sites in the sarcomere at subsaturating fS1 concentrations. There is a 20–200-fold difference in binding constant for rigor S1 between the "on" (open) and "off" (closed) states of actin (Greene et al., 1987; McKillop and Geeves, 1991). This magnitude of difference in binding constants should favor fS1 binding to the "on" sites at low fS1.

DISCUSSION

A characteristic feature of the thin filament is the cooperativity observed in either calcium activation of force in skinned fibers or in S1 binding to reconstituted thin filaments. Some cooperativity can be explained by the structural nature of the thin filament in which one tropomyosin molecule spans seven actin sites. Additional cooperativity has been incorporated into models by invoking inter-unit connectivity between structural units via tropomyosin, yielding a functional unit greater than seven actins (Hill et al., 1980). The functional unit size estimated from biochemical studies was 10–14 actins (Nagashima and Asakura, 1982; Geeves and Lehrer, 1994), whereas some physiological studies have estimated the functional unit size as being the entire length of the thin filament (Brandt et al., 1987). No direct structural measurement has been done on the thin filament to determine the size of the functional unit.

The present work focused upon the relative roles of calcium and myosin heads in activating cross-bridge binding to the thin filament, whereas our previous work (Swartz et al., 1990) focused more upon rigor activation and the role of calcium alone. Interactions of myosin heads with thin filaments have been characterized in both solution and skinned fiber studies, with the observation that binding is a two-step process: initial binding in the weak state ($K_a \approx 10^3$) followed an isomerization to the strong state ($K_a \approx 10^6$) (reviewed by Geeves, 1991). The isomerization constant is about 1 for myosin in the ATP or ADP-P_i state, and it is about 200 for myosin in the ADP or nucleotide-free

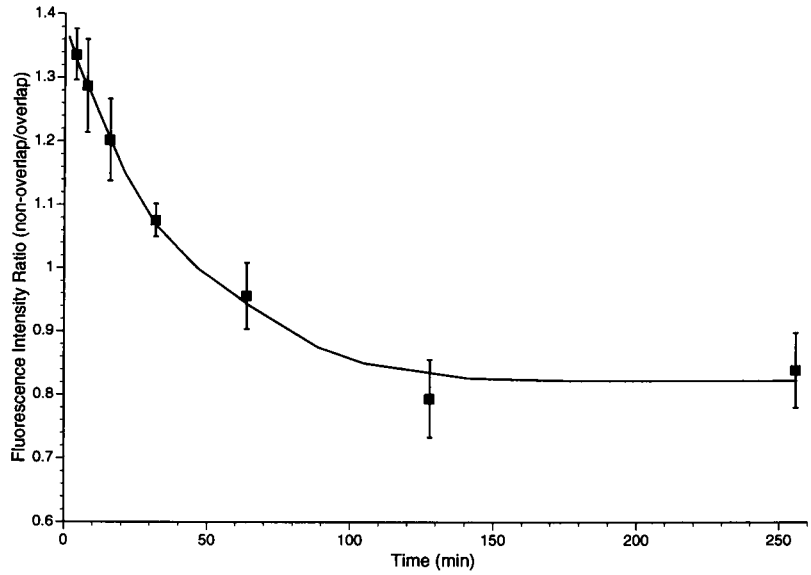

FIGURE 10 Changes in fS1 nonoverlap to overlap intensity ratios with incubation time. Myofibrils were mixed with fS1 [512 A:1 fS1 (2.6 nM)] at pCa 4, and samples were processed for imaging at twofold time intervals starting at 4 min. Fluorescence images were obtained for all time intervals using the same exposure conditions and analyzed for the fluorescence intensity ratio (nonoverlap/overlap) as described in Materials and Methods. Each data point represents the mean (±SD) from 10 myofibrils. Note that the ratio declined during incubation and reached a plateau by 128 min. Thus equilibrium conditions occur sooner than the standard 4-h incubation times used for this study.

(rigor) state. The isomerization from the weak to the strong state involves product release and is thought to result in force production; this transition has been incorporated into a molecular model for the mechanism of force production by the myosin head (Rayment and Holden, 1994). Studies of the binding of strong myosin head states to regulated thin filaments showed that the characteristics of the binding were calcium sensitive (Greene and Eisenberg, 1980). Further analysis of these data led to models in which the thin filament can be in either "off" or "on" states, and the equilibrium between these states is influenced by calcium binding to troponin or by myosin head binding to the thin filament (Hill et al., 1980). This feature was demonstrated in both biochemical (Bremel and Weber, 1972; Nagashima and Asakura, 1982; Lehrer and Morris, 1982; Williams et al., 1988) and structural studies (Swartz et al., 1990).

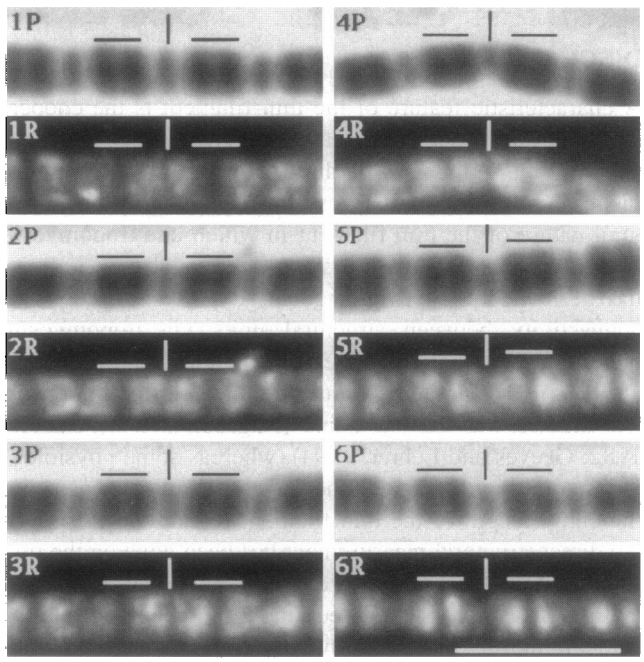

FIGURE 11 Structural look-up table for the intensity ratio change over time measured in Fig. 10. Myofibrils for each time point (except 256 min, which showed distribution identical to that of the 128-min patterns) that were closest to the mean ratio were selected and montaged to show a representative fluorescence image at each time point. Numbers 1–6 represent 4, 8, 16, 32, 64, and 128 min, respectively. Bars and lettering nomenclature are described in the Fig. 2 legend. Note that the changes were subtle between successive time points but are obvious when 4 min is compared to 128 min. These images and the data in Fig. 10 demonstrate that the fS1 redistributes from the nonoverlap to the overlap during incubation under these conditions.

fS1 distribution at high calcium

Previous work showed that calcium resulted in a major change in the pattern of fS1 binding to rigor myofibrils as compared to calcium-free conditions, especially at the low fS1 of that study (Swartz et al., 1990). In the presence of calcium, fS1 was predominantly in the I-band region, with a lower amount in the overlap region; without calcium, most fS1 bound in the overlap region. The patterns depended on the fS1 level: at low levels the patterns of binding differed in the presence and absence of calcium, whereas high levels (about 8A:1 fS1) gave similar patterns at high and low calcium concentrations. In the present study, a wider range of fS1 was used (much lower than our previous study), and different fS1 concentration-dependent patterns were observed compared to the previous study, even at calcium levels that resulted in maximum activation of myofibrillar ATPase activity. Specifically, below 20 nM fS1(64 A:1 fS1), a greater proportion of fS1 was bound in the overlap region than in the nonoverlap region, i.e., ratios were less than 1.0, as shown by the intensity ratio plots in Fig. 7. This was unexpected, considering that the ratio of sites available for binding should be 2:1 if all sites have the same affinity

for fS1. Furthermore, there should be lower accessibility to sites in the overlap region as compared to those in the nonoverlap region. Further analysis of the intensity ratio profile shows a negligible change in the ratio between 0.7 and 5 nM fS1 (2,000 - 256 A:1 fS1), suggesting that within this range fS1 did not perturb the state of activation of the thin filament. These observations are not consistent with the idea that all of the actin sites have the same affinity for fS1 at saturating calcium. Instead, the results support models in which all of the actin sites along the thin filament are not activated in the presence of calcium and in which strong binding of myosin heads to actin is involved in turning on the actin sites, even at high calcium levels (Lehrer, 1994).

Several investigators have modeled the regulation of cross-bridge binding to actin based upon biochemical results. Greene and Eisenberg (1980) measured the equilibrium binding of S1 to regulated thin filaments under a variety of conditions, and these data were subsequently modeled by Hill et al. (1980, 1983). The main feature of these models is that even in the presence of calcium, not all actin sites are in the "on" state; rather, strong binding of some S1 is required to activate all actin sites into the "on" state. Similarly, Lehrer and Morris (1982) showed that the regulated actin-activated ATPase activity of S1 was not maximally activated by calcium at low [S1], and they concluded that calcium alone does not activate all actin sites; instead, full activation requires strong binding of S1. Other studies using a strong binding analog of S1, *N*-ethyl maleimide-modified S1, led to similar conclusions (Nagashima and Asakura, 1982; Williams et al., 1988). Studies using pyrene-labeled tropomyosin demonstrated that there was no tropomyosin conformational change upon calcium binding to regulated thin filaments, but there was a conformational change due to strong binding of S1. Such studies with tropomyosin have led to the proposal that calcium and the myosin head both participate in activating the thin filament, rather than calcium alone (Lehrer, 1994).

More recent studies by Geeves and colleagues have led to a three-state model of the thin filament. To reconcile the different proportions of "off" and "on" states predicted from the equilibrium and kinetic experiments, McKillop and Geeves (1993) proposed that the "off" state can be subdivided into two distinct states: a blocked state and a closed state. More specifically, the model describes three states of the thin filament: a blocked state that cannot readily bind S1, a closed state that binds S1 weakly, and an open state that binds S1 strongly. In the absence of calcium, the blocked state is the predominant form of the thin filament. With calcium, the closed state predominates and the transition from the closed to the open state occurs upon strong binding of S1 and is facilitated by calcium. Kinetic experiments define the relative proportion of structural units in the blocked state but do not distinguish between the closed and open states, whereas equilibrium studies define the relative proportion of structural units in the open state but do not distinguish between closed and blocked states (Head et al., 1995).

Application of this model to the location and relative amounts of fS1 bound to rigor sarcomeres can be used to explain some of the results of the present study. The fS1 is likely to bind only to the open actin sites in the sarcomere. In the overlap region, all available sites will be open independently of calcium, because the ratio of actin to intrinsic rigor heads is 2, and one rigor head can open several actin sites. In the nonoverlap region, the actin sites will either be in the blocked, closed, or open state, depending on the calcium concentration. McKillop and Geeves (1993) predicted that in the presence of calcium, the proportion of the structural units in the different states would be $\leq$0.05 blocked, ~0.8 closed, and ~0.2 open; in the absence of calcium the proportions would be ~0.76 blocked, ~0.22 closed, and $\leq$0.02 open. If all of the nonoverlap actin sites were in the open state (high calcium), then the intensity ratio described in Fig. 7 would be 2 at all ratios of A:fS1. This was not the case at low fS1; instead, the value approached a minimum of about 0.5, in agreement with the value of 0.4 (0.2 open $\times$ 2) predicted by the McKillop and Geeves model for the calcium-saturated thin filament. In the absence of calcium, the minimum value of the ratio was 0.2, considerably greater than the value of 0.04 (0.02 open $\times$ 2) predicted by the model. This difference between model and results likely resides in the method of measurement. There is fluorescence flair, which results in the measured intensity not being restricted to its point source (in this case the overlap region). This is caused by the optical system and the specimen. The contributing factors are the point spread function of the optical system and glare and light scattering within the specimen (Young, 1989). This contributes to the fluorescence intensity measured in the nonoverlap region, in that it does not reach zero even at the Z-line. This is shown in intensity profile curve 1 of Fig. 6 *B*. Some of this error could be decreased by using longer sarcomere lengths and a greater distance between the overlap and nonoverlap windows (ROI). Another possibility is that some fS1 bound to the closed sites and shifted these sites and the adjacent sites into the open state. This seems unlikely because the intensity ratio at low fS1 was essentially linear over an approximately 2-decade range of [fS1]. Considering the major difference in the methods used to develop the model and the methods of the current study, our results readily support the McKillop and Geeves model.

fS1 distribution as a function of [fS1] at high calcium

The distribution of fS1 within the sarcomere at high calcium and different levels of fS1 is shown as images in Fig. 4 and quantitatively in Figs. 6 and 7. At low fS1 binding was favored in the overlap region, whereas increasing levels of fS1 resulted in a gradual increase in the proportion bound in the nonoverlap region. We did not observe this in our previous study, which did not use such low levels of fS1. Fig. 7 shows that the greatest change in the profile occurred

between 10 and 80 nM fS1 (128 - 16 A:1 fS1), suggesting that, within this concentration range, fS1 perturbed the thin filament, i.e., the fS1 appears to have bound to some of the closed sites and shifted them into the open state. This graded change in fS1 distribution was quite distinct from the fS1-induced changes in distribution that occurred at lower calcium. For example, in Fig. 6 *B*, curve 2, the normalized intensity profile shows a distinct peak near the A-band–I-band junction; Fig. 5, 3R, also shows an image of a sarcomere with this type of pattern. Such patterns were not observed at high calcium at any level of fS1. This can be interpreted as the thin filament showing diminished cooperativity in fS1 binding and is in agreement with previous equilibrium and kinetic studies of S1 binding at high calcium (Greene and Eisenberg, 1980; Head et al., 1995; Trybus and Taylor, 1980).

Pattern of fS1 binding as a function of calcium concentration

The distribution of fS1 as a function of calcium is shown in Fig. 5, in which fS1 was 42 nM (32 A:1 fS1) and pCa's were 7.0, 6.0, 5.0, and 4.0. In our previous study, we used only pCa 4.0 and 9.0 and did not investigate the graded response of fS1 distribution as a function of calcium. The current study shows that as calcium concentration increased, there was an increase in the amount of fS1 in the nonoverlap region. The most striking feature in these images is the bright transverse stripe at the A-band–I-band junction at pCa 5.0 (Fig. 5, 3R). This type of distribution was also observed at lower calcium concentration (pCa 6.0 or greater) and higher fS1 concentrations (84–168 nM, 16 - 8 A:1 fS1) and is shown as an intensity profile for pCa 9.0 in Fig. 6 *B*, curve 2. This type of pattern was observed previously (Swartz et al., 1990) and can be explained by the induction of open sites for a short distance into the I-band as a result of intrinsic rigor cross-bridges in the region of overlap. This propagation was presumably caused by fS1 binding to and inducing a state change in the thin filament from the blocked/closed state to the open state. Such a distribution of binding was not likely a result of fS1 first filling all of the sites in the overlap region, because the level of fS1 was $\leq$3% with respect to total sites and the available sites in the overlap region were $\geq$8% of the total sites. Instead, this type of distribution suggests that there is cooperative binding of fS1 along the thin filament, which as pointed out above, was not observed at maximum calcium at any level of fS1.

The apparent cooperativity of fS1 binding can be explained by considering that tropomyosin spans seven actin sites in the structural unit and that the actin sites within this unit are all in the same state. However, there are end-to-end tropomyosin interactions that may increase the size of the functional unit to greater than seven actin sites (Pan et al., 1989), and the flexibility of tropomyosin may decrease the functional unit size (Murray and Weber, 1980). Kinetic studies have led to estimates of 10–14 actin sites per functional unit (Geeves and Lehrer, 1994; Nagashima and Asakura, 1982), in which the binding of one myosin head results in a transition to the open state of five to seven actin sites on each side of the bound myosin head (Geeves and Lehrer, 1994). Previous work on fS1 binding to rigor myofibrils led to the conclusion that the functional unit contains 14 or fewer actins, based upon the restricted binding to fS1 to the overlap region at low calcium (Swartz et al., 1990). The current study supports this idea in that at low calcium (Fig. 3, 1R, Fig. 5, 1R), the fS1 bound solely in the overlap region. A potential difficulty with these estimates of functional unit size is the assumption that all actin sites within the unit have the same properties in terms of S1 binding. Balazs and Epstein (1983) modeled the kinetic data of Trybus and Taylor (1980) on S1 binding to regulated thin filaments using a model in which the actins within a unit did not all have the same properties; instead, this model included short-range, intra-unit cooperativity transmitted by tropomyosin. In their model, binding of S1 is most favored next to an occupied actin site, whereas it is less favored at sites more distant from the occupied site. Their model fit the data well, suggesting that short-range, intra-unit cooperative interactions could explain the properties of the regulated thin filament. This model predicts clustering of bound S1 near the site where the first S1 bound. Clustering of bound fS1 was apparent near the nonoverlap-overlap junction under conditions described in the preceding paragraph. However, clustering as observed in the current study could be explained by either intra- or inter-unit cooperativity because of the limits of resolution of the light microscope.

Relation to thin-filament activation mechanism

One physiological implication of the current work is that the thin filament does not behave in an all-or-none fashion along its entire length, as proposed by Brandt et al., (1987), but shows regional or short-range interactions, even at high levels of calcium. Studies of the distribution of bound calcium by x-ray microanalysis in demembranated rigor muscle fibers showed that more calcium was bound in the overlap region than in the nonoverlap region (Cantino et al., 1993), consistent with the idea that the thin filament displays short-range (2–4 structural units) rather than long-range interactions. The microanalysis study plus other studies using dansyl aziridine-labeled troponin C (Guth and Potter, 1987; Zot and Potter, 1989) delineate another feature of the regulatory system: the effects of calcium binding to troponin C and myosin head attachment to the thin filament are additive.

Recent structural studies of the thin filament at the atomic level have led to the conclusion that the favored position of tropomyosin alone on the actin filament is in a position that blocks the docking of S1 at its actin site (Lorenz et al., 1995). With both tropomyosin and troponin, digital reconstruction of cryoelectron micrographs has led to images that

clearly show a change in the position of tropomyosin upon calcium binding to troponin (Lehman et al., 1994). Analysis of tropomyosin position by x-ray diffraction in oriented regulated actin filaments showed that the degree of movement upon the addition of calcium was less than that observed in intact muscle (Popp and Maéda, 1993), suggesting that additional movement of tropomyosin occurs when it is in the intact filament lattice. This additional movement could be explained by myosin head binding to actin, pushing tropomyosin further into the groove. The results presented in the current paper are consistent with this idea, in that the distribution of fS1 was favored in the overlap region at high calcium when fS1 was very low. Increasing the level of fS1 resulted in binding in both the overlap and nonoverlap regions, suggesting that fS1 itself activated the actin sites in the I-band. Thus the results suggest that a major component of the activation process is strong binding of myosin heads to actin.

This work was supported by the College of Agricultural and Life Sciences, University of Wisconsin–Madison, and by a National Institutes of Health Fellowship to DRS (HL-08400-01) and grants from the National Institutes of Health (HL-25861) to RLM and United States Department of Agriculture (91-37206-6743) to MLG.

REFERENCES

Balazs, A. C., and I. R. Epstein. 1983. Kinetic model for the interaction of myosin subfragment 1 with regulated actin. *Biophys. J.* 44:145–151.

Brandt, P. W., M. S. Diamond, J. S. Rutchik, and F. H. Schachat. 1987. Co-operative interactions between troponin-tropomyosin units extend the length of the thin filament in skeletal muscle. *J. Mol. Biol.* 195: 885–896.

Bremel, R. D., and A. Weber. 1972. Cooperation within actin filament in vertebrate skeletal muscle. *Nature New Biol.* 238:97–101.

Brenner, B. 1988. Effect of Ca^{2+} on crossbridge turnover kinetics in skinned single rabbit psoas fibers: implications for regulation of muscle contraction. *Proc. Natl. Acad. Sci. USA.* 85:3265–3269.

Cantino, M. E., T. StC. Allen, and A. M. Gordon. 1993. Subsarcomeric distribution of calcium in demembranated fibers of rabbit psoas. *Biophys. J.* 64:211–222.

Carter, S. G., and D. W. Karl. 1982. Inorganic phosphate assay with malachite green: an improvement and evaluation. *J. Biochem. Biophys. Methods.* 7:7–13.

Chalovich, J. M. 1992. Actin mediated regulation of muscle contraction. *Pharmacol. Ther.* 55:95–148.

Chalovich, J. M., P. B. Chock, and E. Eisenberg. 1981. Mechanism of action of troponin-tropomyosin. Inhibition of actomyosin ATPase activity without inhibition of myosin binding to actin. *J. Biol. Chem.* 256: 575–578.

Chalovich, J. M., and E. Eisenberg. 1982. Inhibition of actomyosin ATPase activity by troponin-tropomyosin without blocking the binding of myosin to actin. *J. Biol. Chem.* 257:2432–2437.

Fabiato, A. 1988. Computer programs for calculating total from specified free or free from specified total ionic concentrations in aqueous solutions containing multiple metals and ligands. *Methods Enzymol.* 157: 378–417.

Fritz, J. D., D. R. Swartz, and M. L. Greaser. 1989. Factors affecting polyacrylamide gel electrophoresis of high molecular weight myofibrillar proteins. *Anal. Biochem.* 180:205–210.

Geeves, M. A. 1991. The dynamics of actin and myosin association and the crossbridge model of muscle contraction. *Biochem. J.* 274:1–14.

Geeves, M. A., and S. S. Lehrer. 1994. Dynamics of the muscle thin filament regulatory switch: the size of the cooperative unit. *Biophys. J.* 67:273–282.

Godt, R. E., and B. D. Lindley. 1982. Influence of temperature upon contractile activation and isometric force production in mechanically skinned muscle fibers of the frog. *J. Gen. Physiol.* 80:279–297.

Gornall, A. G., C. J. Bardawill, and M. M. David. 1949. Determination of serum protein by means of the biuret reaction. *J. Biol. Chem.* 177: 751–766.

Grabarek, Z., T. Tao, and J. Gergely. 1992. Molecular mechanism of troponin-C function. *J. Muscle Res. Cell Motil.* 13:383–393.

Greene, L. E., and E. Eisenberg. 1980. Cooperative binding of myosin subfragment-1 to the actin-troponin-tropomyosin complex. *Proc. Natl. Acad. Sci. USA.* 77:2616–2620.

Greene, L. E., D. L. Williams, and E. Eisenberg. 1987. Regulation of actomyosin ATPase activity by troponin-tropomyosin: effect of the binding of the myosin subfragment 1 (S1)-ATP complex. *Proc. Natl. Acad. Sci. USA.* 84:3102–3106.

Güth, K., and J. D. Potter. 1987. Effect of rigor and cycling cross-bridges on the structure of troponin C and on the Ca^{2+} affinity of the Ca^{2+}-specific regulatory sites in skinned rabbit psoas fibers. *J. Biol. Chem.* 262:13627–13635.

Haselgrove, J. C. 1973. X-ray evidence for a conformational change in the actin-containing filaments of vertebrate striated muscle. *Cold Spring Harb. Symp. Quant. Biol.* 37:341–352.

Head, J. G., M. D. Ritchie, and M. A. Geeves. 1995. Characterization of the equilibrium between blocked and closed states of muscle thin filaments. *Eur. J. Biochem.* 227:694–699.

Hill, T. L., E. Eisenberg, and L. E. Greene. 1980. Theoretical model for the cooperative equilibrium binding of myosin subfragment 1 to the actin-troponin-tropomyosin complex. *Proc. Natl. Acad. Sci. USA.* 77: 3186–3190.

Hill, T. L., E. Eisenberg, and L. E. Greene. 1983. Alternate model for the cooperative equilibrium binding of myosin subfragment-1-nucleotide complex to actin-troponin-tropomyosin. *Proc. Natl. Acad. Sci. USA.* 80:60–64.

Huxley, H. E. 1973. Structural changes in the actin and myosin containing filaments during contraction. *Cold Spring Harb. Symp. Quant. Biol.* 37:361–376.

Ishii, Y., and S. S. Lehrer. 1987. Fluorescence probe studies on the state of tropomyosin in reconstituted muscle thin filaments. *Biochemistry.* 26: 4922–4925.

Kress, M., H. E. Huxley, A. R. Farqui, and J. Hendrix. 1986. Structural changes during activation of frog muscle studied by time-resolved X-ray diffraction. *J. Mol. Biol.* 188:325–342.

Leavis, P. C., and J. Gergely. 1984. Thin filament proteins and thin filament linked regulation of vertebrate muscle contraction. *CRC Crit. Rev. Biochem.* 16:235–305.

Lehman, W., R. Craig, and P. Vibert. 1994. Ca^{2+}-induced tropomyosin movement in *Limulus* thin filaments revealed by three-dimensional reconstruction. *Nature.* 368:65–67.

Lehrer, S. S. 1994. The regulatory switch of the muscle thin filament: Ca^{2+} or myosin heads. *J. Muscle Res. Cell Motil.* 15:232–236.

Lehrer, S. S., and E. P. Morris. 1982. Dual effects of tropomyosin and troponin-tropomyosin on actomyosin subfragment 1 ATPase. *J. Biol. Chem.* 257:8073–8080.

Lorenz, M., K. J. V. Poole, D. Popp, G. Rosenbaum, and K. C. Holmes. 1995. An atomic model of the unregulated thin filament obtained by X-ray diffraction of oriented actin-tropomyosin gels. *J. Mol. Biol.* 246: 108–119.

McKillop, D. F. A., and M. A. Geeves. 1991. Regulation of the actomyosin subfragment 1 interaction by troponin/tropomyosin. *Biochem. J.* 279:711–718.

McKillop, D. F. A., and M. A. Geeves. 1993. Regulation of the interaction between actin and myosin subfragment 1: evidence for three states of the thin filament. *Biophys. J.* 65:693–701.

Mejbaum-Katzenellenbogen, W., and W. Dobryszycka. 1959. New method for quantitative determination of serum proteins separated by paper electrophoresis. *Clin. Chim. Acta.* 4:515–522.

Moss, R. L. 1986. Effects on shortening velocity of rabbit skeletal muscle due to variations in the level of thin filament activation. *J. Physiol. (Lond.).* 377:487–505.

Murray, J. M., and A. Weber. 1980. Cooperativity of the calcium switch of regulated actomyosin system. *Mol. Cell. Biochem.* 35:11–15.

Murray, J. M., A. Weber, and M. K. Knox. 1981. Myosin subfragment 1 binding to relaxed actin filaments and steric model of relaxation. *Biochemistry.* 20:641–649.

Nagashima, H., and S. Asakura. 1982. Studies on the co-operative properties of tropomyosin-actin and tropomyosin-troponin-actin complexes by the use of *N*-ethylmaleimide-treated and untreated species of myosin subfragment 1. *J. Mol. Biol.* 155:409–428.

Pan, B.-S., A.-M. Gordon, and Z. Luo. 1989. Removal of tropomyosin overlap modifies cooperative binding of myosin S-1 to reconstituted thin filaments of rabbit striated muscle. *J. Biol. Chem.* 264:8495–8498.

Pardee, J. D., and J. A. Spudich. 1982. Purification of muscle actin. *Methods Enzymol.* 85:164–181.

Parry, D. A. D., and J. M. Squire. 1973. The role of tropomyosin in muscle regulation: analysis of the X-ray diffraction patterns from relaxed and contracting muscles. *J. Mol. Biol.* 75:33–55.

Popp, D., and Y. Maéda. 1993. Calcium ions and the structure of muscle actin filament. An X-ray diffraction study. *J. Mol. Biol.* 229:279–285.

Rayment, I., and H. M. Holden. 1994. The three-dimensional structure of a molecular motor. *Trends Biochem. Sci.* 19:129–134.

Rosenfeld, S. S., and E. W. Taylor. 1987. The mechanism of regulation of actomyosin subfragment 1 ATPase. *J. Biol. Chem.* 262:9984–9993.

Squire, J. M. 1994. The actomyosin interaction—shedding light on structural events: "Plus ça change, plus c'est la même chose." *J. Muscle Re. Cell Motil.* 15:227–231.

Swartz, D. R., M. L. Greaser, and B. B. Marsh. 1990. Regulation of binding of subfragment 1 in isolated rigor myofibrils. *J. Cell Biol.* 111: 2989–3001.

Swartz, D. R., M. L. Greaser, and B. B. Marsh. 1993. Structural studies of rigor bovine myofibrils using fluorescence microscopy. II. Influence of sarcomere length on the binding of myosin subfragment-1, alpha-actinin and G-actin to rigor myofibrils. *Meat Sci.* 33:157–190.

Swartz, D. R., and R. L. Moss. 1992. Influence of a strong binding myosin analogue on Ca^{2+}-sensitive mechanical properties of skinned skeletal muscle fibers. *J. Biol. Chem.* 267:20497–20506.

Trybus, K. M., and E. W. Taylor. 1980. Kinetic studies of the cooperative binding of subfragment 1 to regulated actin. *Proc. Natl. Acad. Sci. USA.* 77:7209–7213.

Weeds, A. G., and B. Pope. 1977. Studies on the chymotryptic digestion of myosin. Effects of divalent cations on proteolytic susceptibility. *J. Mol. Biol.* 111:129–157.

Williams, D. L., L. E. Greene, and E. Eisenberg. 1988. Cooperative turning on of myosin subfragment 1 adenosine triphosphatase activity by the troponin-tropomyosin-actin complex. *Biochemistry.* 27:6987–6993.

Yates, L. D., and M. L. Greaser. 1983. Quantitative determination of myosin and actin in rabbit skeletal muscle. *J. Mol. Biol.* 168:123–141.

Young, I. T. 1989. Image fidelity: characterizing the imaging transfer function. *Methods Cell Biol.* 30:1–45.

Zot, A. S., and J. D. Potter. 1987. The effect of $[Mg^{2+}]$ on the Ca^{2+} dependence of ATPase and tension development of fast skeletal muscle. *J. Biol. Chem.* 262:1966–1969.

Zot, A. S., and J. D. Potter. 1989. Reciprocal coupling between troponin C and myosin crossbridge attachment. *Biochemistry.* 28:6751–6756.